

## RESEARCH ARTICLE

10.1002/2017JG004343

## Key Points:

- Molecular formula of leachate DOM from active layer (AL) and permafrost layer (PL) of Qinghai-Tibet Plateau were examined for the first time
- Aromatic C and carbohydrate/protein are preferentially leached out from AL and PL
- The deepening of permafrost thaw induced by global warming will change chemical compositions of leachates

## Supporting Information:

- Supporting Information S1
- Table S1

## Correspondence to:

Y. Xu,  
ypxu@shou.edu.cn

## Citation:

Wang, Y., Xu, Y., Spencer, R. G. M., Zito, P., Kellerman, A., Podgorski, D., et al. (2018). Selective leaching of dissolved organic matter from alpine permafrost soils on the Qinghai-Tibetan Plateau. *Journal of Geophysical Research: Biogeosciences*, 123, 1005–1016. <https://doi.org/10.1002/2017JG004343>







Received 30 NOV 2017

Accepted 3 MAR 2018

Accepted article online 7 MAR 2018

Published online 23 MAR 2018

## Selective Leaching of Dissolved Organic Matter From Alpine Permafrost Soils on the Qinghai-Tibetan Plateau

Yinghui Wang<sup>1,2</sup> , Yunping Xu<sup>1</sup> , Robert G. M. Spencer<sup>3</sup> , Phoebe Zito<sup>4</sup>, Anne Kellerman<sup>3</sup> , David Podgorski<sup>4</sup>, Wenjie Xiao<sup>1,2</sup> , Dandan Wei<sup>1</sup>, Harunur Rashid<sup>1</sup>, and Yuanhe Yang<sup>5</sup> 

<sup>1</sup>Shanghai Engineering Research Center of Hadal Science and Technology, College of Marine Sciences, Shanghai Ocean University, Shanghai, China, <sup>2</sup>Key Laboratory for Earth Surface Processes of the Ministry of Education, College of Urban and Environmental Sciences, Peking University, Beijing, China, <sup>3</sup>National High Magnetic Field Laboratory Geochemistry Group and Department of Earth, Ocean, and Atmospheric Science, Florida State University, Tallahassee, FL, USA, <sup>4</sup>Pontchartrain Institute for Environmental Sciences, Department of Chemistry, University of New Orleans, New Orleans, LA, USA, <sup>5</sup>State Key Laboratory of Vegetation and Environmental Change, Institute of Botany, Chinese Academy of Sciences, Beijing, China

**Abstract** Ongoing global temperature rise has caused significant thaw and degradation of permafrost soils on the Qinghai-Tibetan Plateau (QTP). Leaching of organic matter from permafrost soils to aquatic systems is highly complex and difficult to reproduce in a laboratory setting. We collected samples from natural seeps of active and permafrost layers in an alpine swamp meadow on the QTP to shed light on the composition of mobilized dissolved organic matter (DOM) by combining optical measurements, ultrahigh-resolution Fourier transform ion cyclotron resonance mass spectrometry, radiocarbon (<sup>14</sup>C), and solid-state <sup>13</sup>C nuclear magnetic resonance spectroscopy. Our results show that even though the active layer soils contain large amounts of proteins and carbohydrates, there is a selective release of aromatic components, whereas in the deep permafrost layer, carbohydrate and protein components are preferentially leached during the thawing process. Given these different chemical characteristics of mobilized DOM, we hypothesize that photomineralization contributes significantly to the loss of DOM that is leached from the seasonally thawed surface layer. However, with continued warming, biodegradation will become more important since biolabile materials such as protein and carbohydrate are preferentially released from deep-layer permafrost soils. This transition in DOM leachate source and associated chemical composition has ramifications for downstream fluvial networks on the QTP particularly in terms of processing of carbon and associated fluxes.

### 1. Introduction

Permafrost, the largest component of the terrestrial carbon pool, 1330–1580 Pg C (Pg = 10<sup>15</sup> g) (Schuur et al., 2015), is undergoing rapid degradation due to climate change in the Arctic (Schuur et al., 2011; Serreze & Barry, 2011). Similar to the Arctic, the Qinghai-Tibetan Plateau (QTP), which accounts for approximately 70% of the global alpine permafrost (Bockheim & Munroe, 2014), is also highly sensitive to climate change. Since the 1950s, the average winter temperature of the QTP has risen at a rate of 0.32°C per decade, approximately 3 times the global rate (Liu & Chen, 2000). As permafrost thaws, carbon that was sequestered for thousands of years in permafrost can be mobilized as particulate and dissolved phases into aquatic systems. The dissolved organic matter (DOM) transported to aquatic systems can then be mineralized by microbes and photochemical irradiation (Cory et al., 2014; Drake et al., 2015), and released back to the atmosphere as carbon dioxide (CO<sub>2</sub>) and methane (CH<sub>4</sub>), resulting in a positive feedback with respect to climate change (Schuur et al., 2011; Schuur et al., 2015; Vonk, Tank, Bowden, et al., 2015). Past studies of Arctic systems have suggested that DOM leached from the permafrost layer (PL) has a higher biolability and a lower photolability than DOM leached from the active layer (AL) (Abbott et al., 2014; Mann et al., 2012; Spencer et al., 2015; Vonk, Tank, Mann, et al., 2015; Ward & Cory, 2015). Since the persistence of DOM is largely related to intrinsic chemical composition (Kellerman et al., 2015), detailed characterization of the chemical composition of PL and AL leachates on the QTP is required to understand its fate.

Previous studies have shown that the total potential soil CO<sub>2</sub> emission on the QTP ranges from 737.90–4224.77 g CO<sub>2</sub> m<sup>-1</sup> y<sup>-1</sup>, and thawing-induced CO<sub>2</sub> emissions from permafrost soils would increase general soil respiration by at least about one third on average at a temperature of 5°C (Bosch et al., 2017). A laboratory incubation experiment indicated that the soils from the AL and PL on the QTP had similar

CO<sub>2</sub>-emitting potentials (Chen et al., 2016), while another study suggested that control (nonexposed) soils had significantly higher CO<sub>2</sub> production rates than drape (exposed) soils in a permafrost collapse area on the northern QTP (Mu et al., 2016). Nevertheless, the abundant carbon stock ( $\sim 29.6 \pm 4.2\%$ ; Mu et al., 2016) was lost during the permafrost thaw and collapse processes, potentially from mineralization, leaching, photodegradation, and lateral displacement. A recent study for three Tibetan rivers (the Yellow, Yangtze, and Yarlung Tsangpo) showed that the mean radiocarbon age of DOM was  $511 \pm 294$  years before present (BP) during high flow period (August to September 2014), suggesting the significant export of preaged permafrost carbon into the Tibetan rivers (Qu et al., 2017). Therefore, a better assessment of the permafrost carbon leaching from soil to dissolved phase, as well as transport to fluvial networks is crucial for understanding the carbon cycling on the QTP.

The comparison of DOM chemical compositions between leachates and their parent AL and PL soils can reveal useful information on carbon source, transport, and degradation. This task, however, is challenging because natural DOM comprises thousands of compounds with a large diversity of heterogeneous molecular motifs, intermolecular interactions, and molecular weights. Currently, there are mainly two types of analytical techniques to characterize chemical property of DOM, bulk sample analyses (e.g., UV-visible spectrophotometry and fluorescence spectroscopy) and chemical composition/structure-selective analytical techniques such as Fourier transform ion cyclotron resonance mass spectrometry (FT-ICR MS) and nuclear magnetic resonance spectroscopy (NMR) (Hertkorn et al., 2007; Minor et al., 2014). FT-ICR MS with ultrahigh mass resolution is a powerful tool to examine the molecular-level composition of DOM (Kellerman et al., 2014; Koch & Dittmar, 2006; Stubbins et al., 2010). This comprehensive technique has previously been applied to examine the molecular composition of permafrost-derived DOM in the Arctic (Hodgkins et al., 2016; Stubbins et al., 2017; Ward & Cory, 2016).

In laboratory experiments of soils from Alaska, Ward and Cory (2015) reported the difference in chemical composition of DOM from AL and PL leachates, and Zhang et al. (2017) assessed the effects of lateral flux and percolation of carbon export in tundra soil. These studies provide useful information on the leaching potentials of different DOM components; however, laboratory simulation does not necessarily reflect the natural processes because there are numerous variables (temperature, water content, pH, vegetation cover, etc.) that rapidly change in the environment. Here we collected soils and leachates from the AL and PL in a thermoerosion gully on the northeast QTP during a thawing-freezing cycle. By coupling different concentration (i.e., SPE, ultrafiltration) and analytical techniques (e.g., FT-ICR MS, NMR, radiocarbon age, fluorescence, UV-visible spectroscopy), we conducted detailed characterization of the organic matter composition of permafrost soils and different fractions of DOM from the AL and PL. Our study sought to examine if selective leaching of DOM from AL and PL soils occurred which would have ramifications for biogeochemistry with ongoing climate change.

## 2. Materials and Methods

### 2.1. Site Description

Figure 1a shows the global distribution of permafrost (Brown et al., 2002). Our study area is located in the Gangcha County, northeastern QTP (Figure 1b) and covered by swamp meadow. The regional climate is a typical plateau continental climate with  $\sim 3,000$  h of sunshine annually. Based on the meteorological data from the 2013–2016 (<http://data.cma.cn>), the annual mean temperature and precipitation are 1.01°C and 478.3 mm, respectively. There are three types of grasslands in the QTP, alpine steppe, alpine meadow, and swamp meadow. The coverage of swamp meadow is limited (4.4%) compared to that of alpine steppe and alpine meadow (Yang et al., 2015). However, the high carbon density ( $23.05 \text{ kg C m}^{-2}$ ) makes swamp meadow an important carbon stock, accounting for  $\sim 21.3\%$  of the total organic C in the top 2 m soils in the QTP (Ding et al., 2016). Thus, the degradation of permafrost C in the swamp meadow could cause a considerable carbon release.

In our study area, ice-rich permafrost is thawing and thermokarsts have formed as deep as 220 cm (Figure 1c). This abrupt permafrost thawing can dramatically alter the local landscape, affecting soil, vegetation, and hydrology (Chen et al., 2013). Because of the steep altitude gradient, a number of thermoerosion gullies have developed on a hillslope with an elevation of 3,850 m above sea level (masl). A Ground-Penetrating Radar survey and in situ measurement of an exposed soil profile (Figure 1c) showed that the top 60 cm of the AL

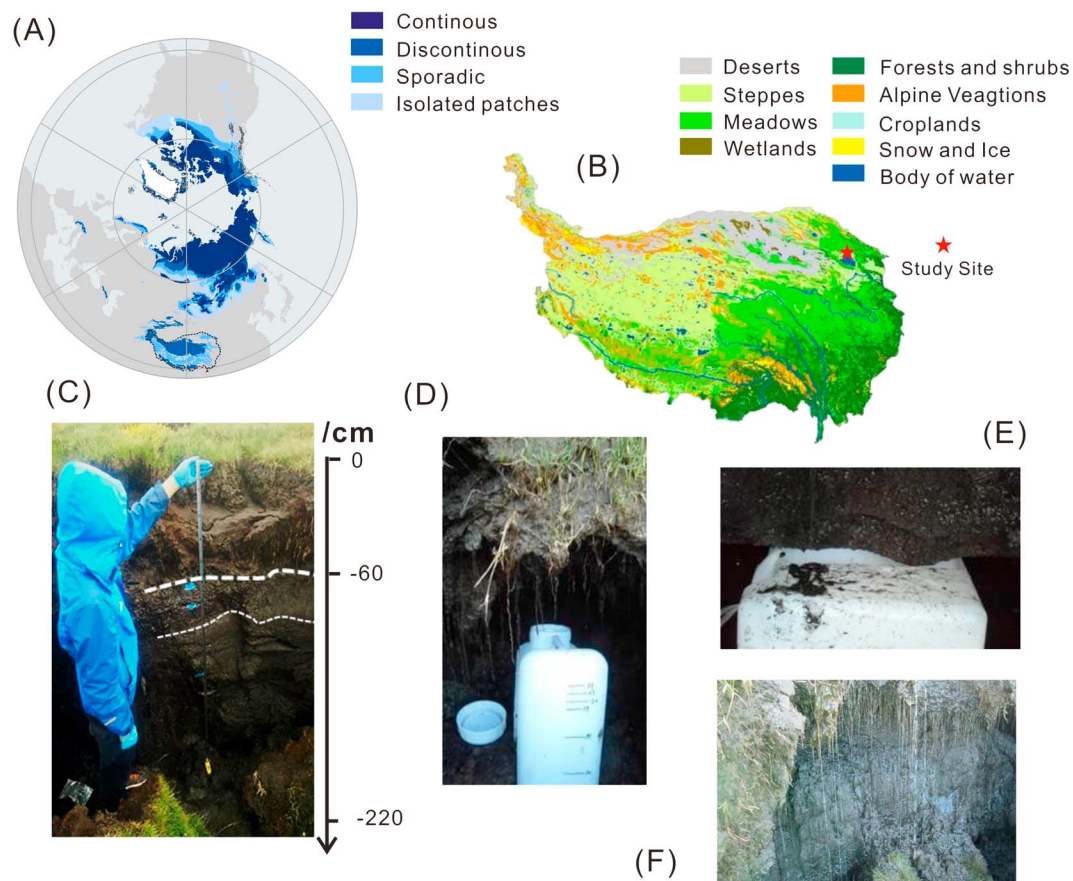


**Figure 1.** (a) Map of the permafrost zones (modified from Brown et al., 2002); (b) study site and distribution of vegetation types throughout the Qinghai-Tibetan Plateau (Chen et al., 2013); (c) a soil profile in the studied thermoerosion gully; (d, e) leachates collected from active layer and permafrost layer; (f) photo showing thermokarst processes.

was composed of abundant litters and roots. The average thaw depth in August 2015 was  $77.7 \pm 2.5$  cm ( $n = 3$ ). Beneath the AL is permafrost soil down to 2 to 3 m (PL) without apparent live or dead plant litters. Because of recent warming, the upper 60 to 68 cm of the PL has partially thawed in summer (a transition zone), below which stable dark-colored permafrost was observed in soil profiles.

## 2.2. Sample Collection and Processing

Sampling was conducted in summer and fall of 2015 and 2016. In total, four types of samples were collected: (i) soils from surface AL (5–15 cm) and PL (180–185 cm); (ii) whole water leached from AL soils (60 cm, Figure 1d) and PL soils (220 cm, Figure 1e); (iii) high molecular weight (HMW) DOM isolated with cross-flow filtration (Millipore regenerated cellulose cassette with 1 k Da cutoff); and (iv) solid phase extracted DOM (SPE-DOM) using the Bond Elut PPL cartridges (Agilent Technologies).

The soil samples were kept on ice and in the dark until brought into the laboratory where they were freeze-dried. The dried soils were passed through 2 mm and 1 mm mesh sieves to remove fine roots, and other residual roots were floated and removed when the soils were treated with HCl or HF before total organic carbon, radiocarbon isotope ( $^{14}\text{C}$ ) and  $^{13}\text{C}$  solid-state NMR analyses.

Leachates from the AL and PL were collected over 2 days to gather  $>15$  L water (100 ml for bulk DOC and optical property analysis; 100 ml for SPE; 12 L for cross-flow ultrafiltration). Water samples were stored in precleaned (alkali, Milli-Q rinsed and acid rinsed before final Milli-Q rinse) HDPE Carboys, and shipped on ice and in the dark to the laboratory. Those water samples were filtered through GF/F 0.7  $\mu\text{m}$  glass fiber filters within 6 h of collection. All glass fiber filters were combusted at 450°C for at least 4 h prior to use.

A portion of the 0.7  $\mu\text{m}$  filtrate was concentrated via a cross-flow ultrafiltration system (Millipore® Pellicon 2 system) to about 1 L. The whole system was cleaned by sequential rinsing with 8 L HCl (0.01 M), 10 L Milli-Q water, 8 L NaOH (0.01 M), and 15 L Milli-Q water between samples. Low molecular weight (LMW) DOM was collected at the beginning, midway, and end of processing to assess ultrafiltration performance by DOC mass balance analysis. Sample retentates were stored at  $-20^{\circ}\text{C}$  and freeze-dried after transported to the laboratory. The freeze-dried HMW DOM was ground into powder with an agate mortar and pestle for chemical and isotopic measurements. The recovery of total DOM was 91.1% and 88.9% for the AL leachate and PL leachate, respectively, while the isolation efficiency of the whole procedure for HMW DOM was 38.1% and 41.5% for the AL leachate and PL leachate, respectively.

The SPE was conducted on the PPL Bond Elut (Agilent Technologies) resins based on Dittmar et al. (2008). Briefly, samples were acidified to pH 2 by analytical grade HCl. To maintain a relatively consistent ionization between samples, aliquot volume was adjusted by initial DOC concentration for a target eluate concentration of  $40\ \mu\text{g C ml}^{-1}$ , and loaded onto 100 mg PPL columns. The cartridges were precleaned with methanol, milli-Q water, and then 0.01 M HCl. After loading samples, the cartridges were flushed with 0.01 M HCl again, and dried with ultrahigh purity  $\text{N}_2$ . The DOM loaded on the PPL column was then eluted with LC-MS grade MeOH (2 ml) and stored at  $-20^{\circ}\text{C}$  until further analysis.

### 2.3. Carbon Concentration

The total organic carbon concentration of the soil samples was measured with an Elementar Vario EL element analyzer after completely removing inorganic carbon by addition of excess 1.0 M HCl. The standard deviation based on the replicate analyses was  $\pm 0.02\%$ . The DOC concentration in the water samples was determined via high-temperature combustion on a Shimadzu TOC-VCPH analyzer. The DOC concentration was calculated as the mean of 3–5 injections and the coefficient of variance across measurements was less than 2% (Mann et al., 2012).

### 2.4. Optical Characterization of Whole Water Leachates

UV-visible absorbance measurements were conducted on a Shimadzu dual beam UV-1800 spectrophotometer between 200 and 800 nm at room temperature. The spectral slope ratio ( $S_{275-295}$ ) was determined by applying log linear fits across the wavelengths 275–295 nm (Helms et al., 2008). Specific UV absorbance at 254 nm ( $\text{SUVA}_{254}$ ) was derived by dividing the decadic absorption coefficient ( $a$ ,  $\text{m}^{-1}$ ) at 254 nm by the DOC concentration ( $\text{L mg C}^{-1} \text{m}^{-1}$ ) (Weishaar et al., 2003).

Fluorescence excitation-emission matrices (EEMs) were collected over an excitation (ex) and emission (em) wavelength of 220–450 nm and 220–550 nm, in 5 and 2 nm increments, respectively. Samples were diluted with Milli-Q water until absorbance was less than 0.3 at 254 nm to prevent inner filter effects. EEMs were corrected for instrument-specific excitation and emission effects and inner filter effects using MatLab R2013a with blank subtraction and Raman normalization. EEMs collected from the surrounding watershed and incubated samples were included in the parallel factor analysis (PARAFAC) data set to increase variability, and three components were identified based on the split-half validation (Stedmon & Bro, 2008). Each of the three components was related to previously identified DOM components (Fellman et al., 2010). The fluorescence index was calculated as the ratio of emission intensity at 470 nm to 520 nm, at an excitation wavelength of 370 nm (Mcknight et al., 2001).

### 2.5. Solid-State $^{13}\text{C}$ NMR Analysis

Soil samples were treated with hydrofluoric acid (10%, v/v) to remove paramagnetic compounds. HMW DOM samples were directly freeze-dried after ultrafiltration to get enough powder for NMR analysis. Pretreated soils and powdered HMW DOM were packed in a 4 mm standard bore CPMAS probe. Solid-state  $^{13}\text{C}$  NMR spectra were obtained using a Bruker BioSpin Avance III 400 MHz WB spectrometer (Changchun Institute of Applied Chemistry, China).

Functional group distributions were quantified by dividing the  $^{13}\text{C}$  NMR spectra into seven chemical shift regions: 0–45 ppm for alkyl C, 45–60 ppm for N-alkyl C and methoxyl groups, 60–95 ppm for O-alkyl C, 95–110 ppm for di-O-alkyl C, 110–145 ppm for aromatic C, 145–165 ppm for phenolic C, and 165–210 ppm for carboxyl groups (Nelson & Baldock, 2005). Spectra processing was quantified by using Mnova NMR software (Metrelab Research). Although different types of biomolecules could be separated within the chemical

**Table 1**  
Bulk Organic Matter Characteristics of Soil Profiles and Optical Property of AL and PL Leachates

Type	Parameter	AL	PL	PL
Soils	Depth (cm)	10	65	180
	Total organic carbon (%)	22.81	12.79	4.85
	C/N	13.97	18.86	16.38
	$\Delta^{14}\text{C}$ (‰)	120.10	-540.60	-650.90
	$^{14}\text{C}$ age (BP)	> Modern	6250	8455
Leachates	DOC (mg C L <sup>-1</sup> )	12.34	-	111.60
	SUVA <sub>254</sub> (L mg C <sup>-1</sup> m <sup>-1</sup> )	3.69	-	0.85
	$S_{275-295}$ ( $\times 10^{-3}$ nm <sup>-1</sup> )	14.15	-	18.99
	Fluorescence index	1.55	-	1.72
	Component 1 (%)	49.20	-	41.83
	Component 2 (%)	38.57	-	25.60
	Component 3 (%)	12.22	-	32.57

shift regions of NMR spectra (Sjögersten et al., 2003; Ward & Cory, 2015), the overlap of C types in adjacent regions exists. Considering this, we applied a combined  $^{13}\text{C}$  NMR, N/C, and the biomolecular mixing model developed by Nelson and Baldock (2005) to calculate the proportion of each type of molecular compositions: carbohydrate, protein, lignin, aliphatic material, carbonyl, and char.

## 2.6. FT-ICR MS Analysis

SPE-DOM was analyzed on a 9.4 tesla custom-built FT-ICR MS at the National High Magnetic Field Laboratory (NHMFL; Tallahassee, FL; Kaiser et al., 2011). Negatively charged molecular ions were generated with an electrospray ionization (ESI) source. Samples were injected at 0.7  $\mu\text{L}/\text{min}$ , and 100 broadband scans were accumulated for each mass spectra. MIDAS Predator Analysis and Molecular Formula Calculator software from the NHMFL were used for internal calibration and molecular formula assignment, respectively. Signals from  $m/z$  150 to

1,500  $> 6\sigma$  RMS baseline noise were considered for assignment. Molecular formulas within a  $\pm 0.5$  ppm error range were calculated based on the presence of carbon, hydrogen, oxygen, nitrogen, and sulfur.

Formulas assigned with EnviroOrg<sup>™</sup> software were categorized by compound class based on the elemental composition of molecular formulas (Spencer et al., 2014). The groups referred in this study are delineated by the modified aromaticity index ( $\text{Al}_{\text{mod}}$ ; Koch & Dittmar, 2006), H/C, O/C, and elemental composition as in Kellerman et al. (2015).  $\text{Al}_{\text{mod}}$  values 0.5–0.66 and  $>0.66$  were assigned as polyphenols and condensed aromatics, respectively (Koch & Dittmar, 2006). Further groups were defined as phenolic and unsaturated compounds, aliphatic compounds, peptides, and sugars. Polyphenols are mainly derived from vascular plants, but microbial-derived polyphenolic compounds are also possible. Condensed aromatics are more likely black carbon materials, whereas the aliphatic, highly unsaturated aliphatic, and phenolic compounds have more ambiguous sources. The relative abundance of these defined groups was weighted by signal magnitude, which was normalized to the sum of all signals in each spectrum.

## 2.7. Carbon Isotopic Analyses

Radiocarbon isotopes ( $^{14}\text{C}$ ) of pretreated soils and powdered HMW DOM were analyzed at the Keck Carbon Cycle Accelerator Mass Spectrometer at University of California, Irvine. Radiocarbon concentrations are given as fractions of the modern standard,  $\Delta^{14}\text{C}$ , and conventional radiocarbon age, following the conventions of Stuiver and Polach (1977). Sample preparation backgrounds were subtracted based on measurements of  $^{14}\text{C}$ -free coal.

## 3. Results and Discussion

### 3.1. Organic Carbon Concentration and Age Difference Between AL and PL

The organic carbon percentage decreases with the depth in the soil profile (Table 1). At the surface AL (5–15 cm), the amount of organic carbon is 22.81%, and down to 65 cm, it drops to 12.79%. At the bottom of the permafrost soil examined (180 cm deep), the organic carbon decreased to 4.85%. The higher concentration of organic carbon in the AL than the PL observed in our study is comparable to the trend reported in the Arctic (Dutta et al., 2006; Pries et al., 2012; Waldrop et al., 2010) and European alpine permafrost (Frey et al., 2016). Such a depth pattern was attributed to fresh organic carbon input to the AL and a higher degree of organic carbon degradation in the PL (Grewer et al., 2016).

The permafrost soil at 180 cm depth has a  $^{14}\text{C}$  age of  $8400 \pm 25$  years BP, while the soil at 65 cm depth has a  $^{14}\text{C}$  age of  $6250 \pm 20$  years BP, indicating a high deposition rate (52 cm/thousand years) in the early to mid-Holocene. Previous studies reported that the present distribution of the QTP permafrost developed under the changing climate in the Holocene (Jin et al., 2006; Wang, 1989; Zhang, 1981). During the Early Holocene (8500–7000 years BP), permafrost remnants from the last glaciation were significantly degraded, but large amounts of Holocene peat and humus were produced (Jin et al., 2006), consistent with the high deposition rate between 8400– and 6250 years BP determined in our study.

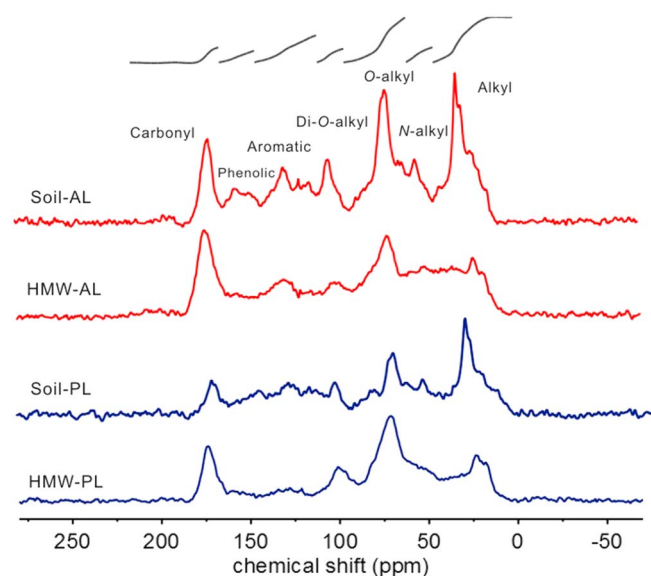


**Figure 2.** Solid-state CPMAS <sup>13</sup>C NMR spectra of soils (Soil-*n*) and HMW DOM (HMW-*n*) from the active layer and PL. The chemical shift regions 0–45, 45–60, 60–95, 95–110, 110–145, 145–165 and 165–210 ppm refer to alkyl, O-alkyl C, N-alkyl, di-O-alkyl C, aromatic, phenolic, and carbonyl, respectively.

### 3.2. Organic Carbon Components of AL and PL Soils Revealed by <sup>13</sup>C NMR

Figure 2 shows solid-state CPMAS <sup>13</sup>C NMR spectra of selected soils and HMW DOM from the AL and PL, with the relative abundance of major C functional groups listed in Table 2. Organic carbon in surface AL soil is dominated by alkyl C (24.5%) and O-alkyl C (24.0%), followed by aromatic C (16.1%) and carbonyl C (11.6%). Other types of C (protein and char) are less than 10%. With increasing depth in the PL, the contribution of alkyl C to total organic carbon increases to 30.5%, and O-alkyl C and aromatic C decrease to 22.0% and 18.0%, respectively. The remaining C groups such as N-alkyl C, char, and protein have a similar abundance (6.5%–8.5%).

The permafrost soils from the QTP contains relatively higher alkyl C contribution than the Arctic soils, particularly those from deep PL (Ejarque & Abakumov, 2016; Mueller et al., 2015; Pautler et al., 2010; Sjögersten et al., 2016). This difference is likely related to overlying vegetation types and degradation stage of the soil organic matter (SOM). It is well known that the surface organic matter inputs determine the quantity and quality of the SOM (Jobbágy & Jackson, 2000; Lal, 2005). Our study area is covered by an alpine swamp meadow dominated by graminoids and sedges (Chen et al., 2016), whereas the high-latitude permafrost regions have vegetation dominated by

mosses, dwarf shrubs, and coniferous trees (Hobbie et al., 2000). The degradation of plant-derived compounds promotes higher alkyl/O-alkyl C values (Pautler et al., 2010; Sjögersten et al., 2003). Relatively higher values for alkyl/O-alkyl C in our study (1.02 and 1.39 for AL and PL soils, respectively) indicate that the SOM in the QTP has experienced more severe degradation than that in the Arctic (0.47 and 0.66 for AL and PL in average, *n* = 12 and 4, Table S1 in the supporting information), likely due to higher annual mean temperature in most areas of the QTP than examined in past Arctic focused studies (Maxwell, 1992).

### 3.3. Chemical Compositions of Bulk DOM, HMW DOM, and SPE-DOM From AL and PL

#### 3.3.1. Optical Properties of Leachate DOM

The composition of the chromophoric and fluorescent DOM is quite different between the AL leachate and PL leachate from the QTP (Table 1). Generally, the AL leachate has a much higher SUVA<sub>254</sub> (3.69 L mg C<sup>-1</sup> m<sup>-1</sup>) and a lower S<sub>275–297</sub> (14.15 × 10<sup>-3</sup> nm<sup>-1</sup>) compared with the PL leachate (0.85 L mg C<sup>-1</sup> m<sup>-1</sup> and 18.99 × 10<sup>-3</sup> nm<sup>-1</sup>), reflecting that DOM leached from the AL is composed of predominantly aromatic, HMW compounds relative to DOM leached from the PL. In addition, the fluorescence index is higher for the PL leachate compared with the AL leachate (1.72 versus 1.55; Table 1), again denoting that the PL leachate is composed of more aliphatic DOM derived from a microbial source (Mcknight et al., 2001).

The PARAFAC modeling of EEMs spectra includes three components (Table 1), with two (C1, C2) categorized as humic-like components and one (C3) as a protein-like component. C1 and C2 display spectra closely related to the classic peaks defined as “C” and “A” (Coble, 1996), suggesting a source of vascular plants or

**Table 2**  
Relative Abundance of Functional C Groups in Soils and HMW DOM From the PL and AL Leachates

Chemical shift regions (ppm)	Functional groups	Typical compounds	SOM		HMW DOM	
			AL	PL	AL	PL
0–45	Alkyl	Lipid, protein	24.5	30.5	22.2	21.8
45–60	N-alkyl/methoxy	Protein, lignin	8.4	8.5	9.8	10.2
60–95	O-alkyl	Carbohydrate	24.0	21.9	23.5	33.8
95–110	Di-O-alkyl	Carbohydrate, lignin	7.9	6.5	6.5	8.1
110–145	Aromatic	Lignin, char	16.1	18.0	14.2	8.0
145–165	O-aromatic	Lignin, char	7.5	7.0	6.6	4.3
165–215	Carbonyl	Char, protein	11.6	7.6	17.1	13.8

soil-derived DOM (Coble, 1996; Fellman et al., 2010). The relative contribution of C1 and C2 is higher in the AL leachate than that in the PL leachate, and C1 is the dominant fluorophore in both layers (Table 1), suggesting vascular plants and soils as major carbon sources for all leachates. However, the protein-like component C3 has a higher proportion in the PL leachate. A similar composition pattern of C1, C2, and C3 was observed in Arctic permafrost DOM (Abbott et al., 2014; Vonk, Tank, Mann, et al., 2015; Ward & Cory, 2015), indicating that the PL leachate DOM might have higher bioavailability than the AL leachate DOM on the QTP, as that observed in high-latitude permafrost. Overall, the optical properties suggest that the DOM leached from the AL leachate is enriched in aromatic, high molecular weight (MW) compounds that are primarily derived from soil or plant organic matter, while the DOM leached from the PL is composed of aliphatic, low MW DOM that is predominantly derived from a microbial source. Since the intrinsic molecular properties are an important control on overall organic matter reactivity (Kellerman et al., 2015), different chemical compositions between the PL and AL leachates likely influence the bioavailability of mobilized DOM in downstream waters, and thus affect food and nutrient availability in these receiving ecosystems.

### 3.3.2. $^{13}\text{C}$ NMR Characterization of HMW DOM

The solid-state  $^{13}\text{C}$  NMR spectra reveals compositional differences in the HMW DOM from the AL and PL leachates (Table 2). Alkyl C is the dominant C type in SOM (24.5% in AL, 30.5% in PL), while the O-alkyl C is the most enriched structural group in HMW DOM, representing 23.5% in the AL and 33.8% in the PL. Despite an apparent decrease, alkyl C is still an important functional group in HMW DOM, accounting for 22.2% in the AL and 21.8% in the PL. Besides alkyl C and O-alkyl C, carbonyl C is another important component of HMW DOM in the AL leachate (17.1%) and the PL leachate (13.8%). HMW DOM has a lower fraction of aromatic C (14.2% in the AL leachate and 8.0% in PL leachate) than the SOM (16.1% in AL and 18.0% in PL). In addition, both SOM and HMW DOM have minor contributions from N-alkyl C, di-O-alkyl C, and phenolic C, and only the contribution of N-alkyl C is slightly higher in the HMW DOM than in the SOM (9.8 versus 8.5% in AL and 10.2 versus 8.5% in PL).

The relative abundances of functional groups are different between HMW DOM and SOM even from the same layer; however, major C groups in HMW DOM from different layers have the same order of magnitude (O-alkyl C > alkyl C). Such a pattern is different with that of SPE-DOM from the Imnavait Creek watershed on the North Slope of Alaska that comprised more abundant alkyl C than O-alkyl C (Ward & Cory, 2015). We attribute this difference to different chemical compositions of SOM between the QTP and the Alaskan Arctic. However, the extraction bias between SPE (enriched for LMW) and cross-flow UF (enriched for HMW) could not be excluded at the current stage since the samples for  $^{13}\text{C}$  NMR analyses are SPE-DOM in Ward and Cory (2015) and UF-DOM in our work. Carbonyl C is the third most abundant functional group for both the AL and PL leachates. For the remaining C groups, aromatic C and O-aromatic C comprise a total of 20.8% in the AL as opposed to only 12.3% in the PL. A larger fraction of aromatic and O-aromatic C in the AL HMW DOM, as well as in the AL whole DOM fluorescence suggests that the AL leachate in general has higher aromaticity, which is attributed to a selected release of aromatic compounds from the AL soils.

### 3.3.3. Characterization of SPE-DOM Based on FT-ICR MS

The FT-ICR MS data reveal the compositional difference between the DOM leached from the AL relative to the PL. To visualize the differences, van Krevelen diagrams were plotted for all samples and five compound classes were identified according to elemental compositions (e.g., H/C, O/C; Figure 3) with their relative abundance summarized in Table 3. The SPE-DOM from AL and PL leachates contain 14,709 and 9,645 assigned molecular formulas. The PL SPE-DOM is more enriched in unsaturated compounds (74.2%) and has a higher proportion of biolabile components than that of the AL DOM including aliphatic compounds (7.9% versus 1.2%) and peptide-like compounds (2.1% versus 0.1%; Table 3). Past studies have shown high biolability for these compounds in Arctic permafrost-derived DOM focused studies (Spencer et al., 2015). The detailed FT-ICR MS classification of SPE-DOM shows that the higher aromaticity of the AL leachate is likely attributed to the higher percentage of condensed aromatics and polyphenolic compounds, consistent with the  $\text{SUVA}_{254}$  of the leachates and  $^{13}\text{C}$  NMR data of HMW DOM and SOM (see section 3.2). The higher MW of the AL leachate DOM is confirmed by the FT-ICR MS data as the peak intensity weighted mean mass of AL SPE-DOM is 46 Da higher than PL SPE-DOM (498 versus 452 Da), which is again consistent with the results from the optical measurement (e.g.,  $S_{275-295}$ ).

More differences between the AL and PL leachates are evident when assessing the unique molecular formulas (Figures 3 and S1). Nearly 32% of the assigned formulas detected are unique to either the AL and PL

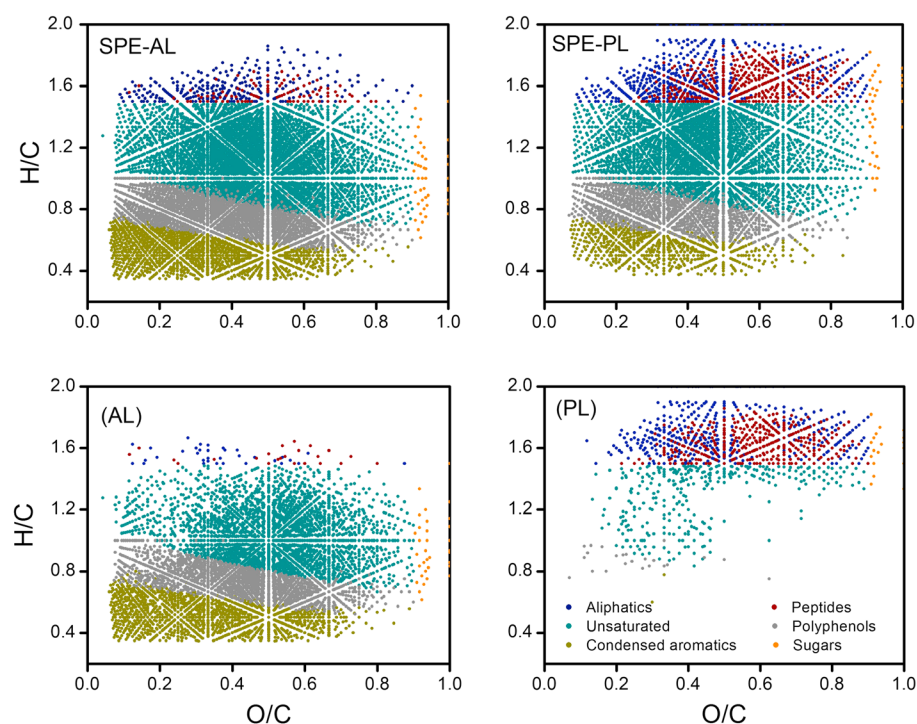


**Figure 3.** Van Krevelen diagrams of DOM leachates (SPE-AL, SPE-PL) and the unique molecular formulas found solely in leachates from active layer (AL) and permafrost layer (PL). Color indicates compound categories.

leachates, with 26% detected only in the AL SPE-DOM, and 6% only in the PL SPE-DOM. The van Krevelen diagrams reveal that most of the formulas unique to the AL leachate DOM are polyphenolic and condensed aromatic compounds, while those unique to the PL leachate are more aliphatic and peptides. The remaining 68% of assigned elemental formulas are present in both the AL and PL leachate DOM, but their Spearman's rank correlation (0.38,  $P < 0.01$ ) is weak between the AL and PL leachates. Furthermore, compounds containing N and S are only detected in the AL leachate DOM. Overall, the AL DOM is more aromatic in character, with a higher molecular richness, whereas the PL DOM has a lower mean mass and higher fraction of aliphatic and peptide-like compounds.

### 3.4. Selective Leaching of DOM From PL and AL on the QTP

The recovery of the isolation steps (i.e., SPE and UF) inevitably inhibits our understanding of the chemical composition of DOM as a whole. In order to circumvent this problem, we combine these different concentration and isolation steps with the FT-ICR MS and NMR analyses, as well as with optical analyses without any pretreatment to provide as holistic an overview as possible. With a relatively full picture of DOM and by comparing the AL and PL soils, we have an opportunity to obtain a comprehensive view of the leaching process on the QTP permafrost region. By applying the biomolecular mixing model developed by Nelson and Baldock (2005), we calculated the relative abundance of six major molecular components (i.e., carbohydrate, protein, lignin, aliphatic material, char, and carbonyl) based on  $^{13}\text{C}$  NMR spectra and N/C. The results show that the SOM from the AL has a slightly larger portion of protein (27%), closely followed by carbohydrate (25%) and

**Table 3**

The Number of Assigned Molecular Formulas to Each Defined Compound Class and Relative Abundance as Revealed by FT-ICR MS for SPE-DOM From AL and PL Leachates on the QTP

Sample	Formulas assigned	Mean mass	Condensed aromatics (%)	Polyphenols (%)	Unsaturated O/C < 0.5 (%)	Unsaturated O/C > 0.5 (%)	Aliphatics (%)	Peptides (%)
SPE-AL	14709	498.81	2,543 (17.2%)	3,304 (27.1%)	4,288 (22.9%)	3,866 (31.4%)	536 (1.2%)	117 (0.1%)
SPE-PL	9645	452.73	925 (4.3%)	1,607 (11.3%)	3,260 (32.5%)	2,242 (41.7%)	1,095 (7.9%)	479 (2.1%)

Note. The relative abundance of each group was weighted by peak intensity.



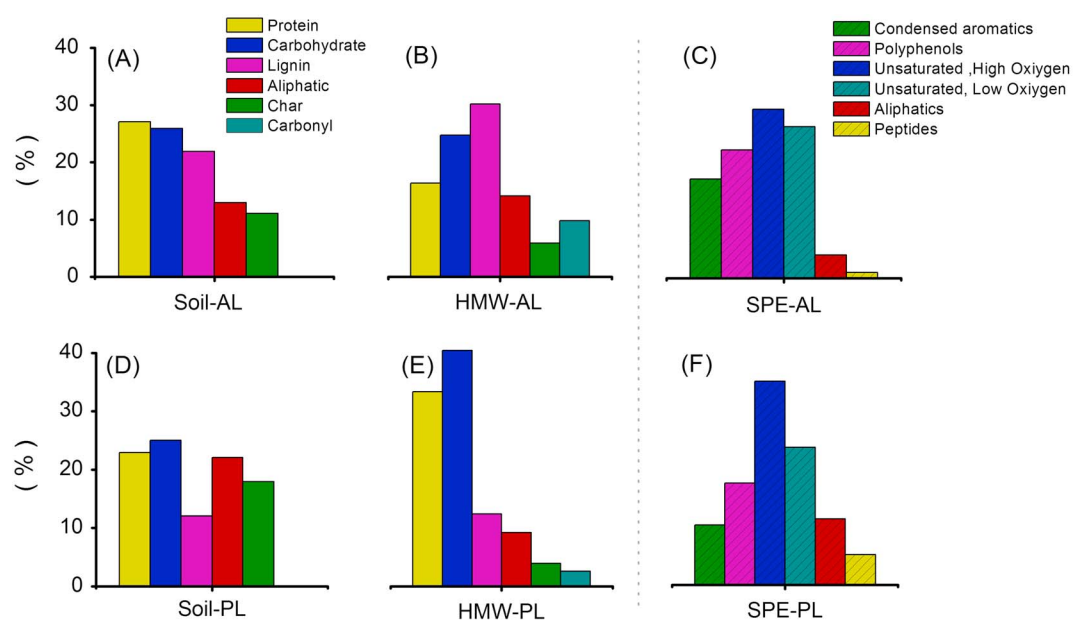


**Figure 4.** The bimolecular composition of the (a, d) (Soil-*n*) and the (b, e) HMW fraction of DOM revealed by  $^{13}\text{C}$  NMR, (c, f) compound class of the LMW portion of DOM (SPE-*n*) revealed by FT-ICR MS.

lignin (21%), whereas the rest of the SOM are mostly aliphatics and char (Figure 4a). However, the HMW fraction of the DOM released from the AL has a high contribution from lignin (29%; Figure 4b). While the majority of molecular formulas identified by FT-ICR MS are classified as unsaturated and phenolic compounds in LMW DOM of the AL leachate (54%), aromatic material (e.g., condensed aromatic compounds and polyphenolic compounds) are still an important part of the carbon composition (39%; Figure 4c).

We defined an enrichment factor to express the degree of selected leaching of DOM, which is expressed as a ratio of aromatic C abundance in leachate DOM to that in source SOM ( $E_c = \frac{\sum \text{aromatic C in leachate DOM}}{\sum \text{aromatic C in source soil}}$ ). We assume that the sum of SPE-DOM (most LMW) and UF-DOM (most HMW) represents whole leachate DOM considering that the extraction efficiency of permafrost-derived DOM is ~40% for UF (this study) and ~60% for PPL-SPE (Ward & Cory, 2015). Since UF-DOM and SPE-DOM were analyzed by  $^{13}\text{C}$  NMR and FT-ICR MS, respectively, which inevitably resulted in the selectivity of certain components of DOM. The  $^{13}\text{C}$  NMR is sensitive to the presence of aliphatic carbon, but often underestimates the amount of aromatic and particularly, of carbonylic (carboxylic) carbon (Love et al., 1992), whereas FT-ICR MS, which uses ESI for ionization of the analyte, is sensitive to easily ionizable, carboxyl-containing molecules, but only partially detects poorly ionizable carbohydrates or other similar moieties (Hodgkins et al., 2016). Despite these weaknesses, the  $E_c$  is still a useful indicator for estimating selectivity of SOM during leaching process.

Using the extraction efficiency of UF (40%) and SPE (60%),  $^{13}\text{C}$  NMR and FT-ICR MS data (Table 2 and Figure 4), the calculated  $E_c$  is 1.34 for the AL leachate. Therefore, even though the AL soils have a large fraction of proteins and carbohydrates, lignin and aromatic material are preferentially leached out of the soils over other components, which contribute to the higher aromaticity of the AL leachate (34% greater than source SOM).

For PL soils, carbohydrate, protein, aliphatics, and char had relatively similar proportions, which were 24%, 23%, 22%, and 18%, respectively, while the contribution of lignin was only 12% (Figure 4d). The HMW portion of the DOM had a high abundance of proteins (33%) and carbohydrates (40%; Figure 4e). Even though these biopolymer fractions tend to accumulate in the HMW fraction, the LMW fraction of PL leachate also had a higher proportion of aliphatic compounds and peptide-like compounds than the AL leachate (16% versus 5%; Figures 4c and 4f). According to the relative abundance of lignin and char, the calculated  $E_c$  is 0.84 for the PL leachate, confirming that aromatic carbon was preferentially retained in PL soil relative to other C components (16% lower in leachate DOM than source SOM). Overall, the DOM leached from the AL and PL on the QTP was composed of more aromatic and aliphatic components, respectively, relative to the corresponding

source soils. The reason for this selective leaching of permafrost SOM is not known, but a strong binding of aromatic C to minerals particularly Fe oxides in the hypoxic PL (Wang et al., 2017) may be an important mechanism. A study for different density fractions of permafrost soils is necessary to understand the distribution of aromatic C in free and mineral-bound forms. Nevertheless, our multiple lines of evidence showed different leaching behaviors of aromatic C between AL and PL. This selected leaching from thawed permafrost likely plays an important role in carbon cycling in downstream environments because aromatic-enriched DOM is more sensitive to photodegradation, while carbohydrate/protein-enriched DOM is more biolabile to microbes (Cory et al., 2014; Obernosterer & Benner, 2004).

#### 4. Summary

By applying complimentary analytical methods (i.e., FT-ICR MS,  $^{13}\text{C}$  NMR, radiocarbon age, fluorescence, and UV-visible optical analyses), we obtained a unique insight into the DOM leachates from a thermokarst gully in the swamp meadow of the QTP. Several lines of evidence suggest preferential leaching of aromatic compounds from the AL and selective leaching of proteins and carbohydrates from the PL. Considering that currently there is a seasonal thaw of the entire AL but only a partial thaw of the PL on the QTP, we postulate that photomineralization of aromatic C-enriched DOM is currently an important pathway with respect to C fate (Cory et al., 2014). However, as the QTP is undergoing continued warming, the deeper, currently frozen permafrost soils will be thawed, leading to more biolabile material (e.g., carbohydrate and protein) to be mobilized, and supply “new” nutrient and energy sources to downstream ecosystems. On all accounts, the abundant permafrost-leached C from the swamp meadow will be returned to the atmosphere quickly as  $\text{CO}_2$  and  $\text{CH}_4$ , and thereby lead to a positive feedback to climate change, although its magnitude is unknown currently. The next step will examine permafrost leaching in alpine steppe and alpine meadow to obtain a full picture of permafrost C dynamics in this world’s largest and highest plateau.

#### Acknowledgments

The data set for this study is available at <https://doi.org/10.6084/m9.fig-share.5649232.v1>. The National Basic Research Program of China supported this research work (grant 2014CB954001). We thank the China Scholarship Council for supporting the first author’s study in Florida State University (U.S.A.). We are grateful to Futing Liu, Yanyan Yan, Shangzhe Zhou, and Xinyu Zhang for assistance in the fieldwork. We also thank Yingxun Du and Wei He for providing the manuscript on PARAFAC method. FT-ICR MS was supported by NSF (DMR-1157490).

#### References

- Abbott, B. W., Larouche, J. R., Jones, J. B., Bowden, W. B., & Balsler, A. W. (2014). Elevated dissolved organic carbon biodegradability from thawing and collapsing permafrost. *Journal of Geophysical Research: Biogeosciences*, *119*, 2049–2063. <https://doi.org/10.1002/2014JG002678>
- Bockheim, J. G., & Munroe, J. S. (2014). Organic carbon pools and genesis of alpine soils with permafrost: A review. *Arctic, Antarctic, and Alpine Research*, *46*(4), 987–1006. <https://doi.org/10.1657/1938-4246-46.4.987>
- Bosch, A., Schmidt, K., He, J. S., Doerfer, C., & Scholten, T. (2017). Potential  $\text{CO}_2$  emissions from defrosting permafrost soils of the Qinghai-Tibet plateau under different scenarios of climate change in 2050 and 2070. *Catena*, *149*, 221–231. <https://doi.org/10.1016/j.catena.2016.08.035>
- Brown, J., Ferrians, J. O. J., Heginbottom, J. A., & Melnikov, E. S. (2002). *Circum-Arctic Map of Permafrost and Ground Ice Conditions (Version 2)*. Boulder, CO: National Snow and Ice Data Center/World Data Center for Glaciology.
- Chen, L., Liang, J., Qin, S., Liu, L., Fang, K., Xu, Y., et al. (2016). Determinants of carbon release from the active layer and permafrost deposits on the Tibetan Plateau. *Nature Communications*, *7*, 13046. <https://doi.org/10.1038/ncomms13046>
- Chen, H., Zhu, Q., Peng, C., Wu, N., Wang, Y., Fang, X., et al. (2013). The impacts of climate change and human activities on biogeochemical cycles on the Qinghai-Tibetan plateau. *Global Change Biology*, *19*(10), 2940–2955. <https://doi.org/10.1111/gcb.12277>
- Coble, P. G. (1996). Characterization of marine and terrestrial DOM in seawater using excitation-emission matrix spectroscopy. *Marine Chemistry*, *51*(4), 325–346. [https://doi.org/10.1016/0304-4203\(95\)00062-3](https://doi.org/10.1016/0304-4203(95)00062-3)
- Cory, R. M., Ward, C. P., Crump, B. C., & Kling, G. W. (2014). Carbon cycle. Sunlight controls water column processing of carbon in arctic fresh waters. *Science*, *345*(6199), 925–928. <https://doi.org/10.1126/science.1253119>
- Ding, J., Li, F., Yang, G., Chen, L., Zhang, B., Liu, L., et al. (2016). The permafrost carbon inventory on the Tibetan plateau: A new evaluation using deep sediment cores. *Global Change Biology*, *22*(8), 2688–2701. <https://doi.org/10.1111/gcb.13257>
- Dittmar, T., Koch, B., Hertkorn, N., & Kattner, G. (2008). A simple and efficient method for the solid-phase extraction of dissolved organic matter (SPE-DOM) from seawater. *Limnology and Oceanography: Methods*, *6*(6), 230–235. <https://doi.org/10.4319/lom.2008.6.230>
- Drake, T. W., Wickland, K. P., Spencer, R. G., McKnight, D. M., & Striegl, R. G. (2015). Ancient low-molecular-weight organic acids in permafrost fuel rapid carbon dioxide production upon thaw. *Proceedings of the National Academy of Sciences of the United States of America*, *112*(45), 13,946–13,951. <https://doi.org/10.1073/pnas.1511705112>
- Dutta, K., Schuur, E. A. G., Neff, J. C., & Zimov, S. A. (2006). Potential carbon release from permafrost soils of northeastern Siberia. *Global Change Biology*, *12*(12), 2336–2351. <https://doi.org/10.1111/j.1365-2486.2006.01259.x>
- Ejarch, E., & Abakumov, E. (2016). Stability and biodegradability of organic matter from Arctic soils of western Siberia: Insights from  $^{13}\text{C}$ -NMR spectroscopy and elemental analysis. *Solid Earth*, *7*(1), 153–165. <https://doi.org/10.5194/se-7-153-2016>
- Fellman, J. B., Hood, E., & Spencer, R. G. M. (2010). Fluorescence spectroscopy opens new windows into dissolved organic matter dynamics in freshwater ecosystems: A review. *Limnology and Oceanography*, *55*(6), 2452–2462. <https://doi.org/10.4319/lo.2010.55.6.2452>
- Frey, B., Rime, T., Phillips, M., Stierli, B., Hajdas, I., Widmer, F., & Hartmann, M. (2016). Microbial diversity in European alpine permafrost and active layers. *FEMS Microbiology Ecology*, *92*(3), fiv018. <https://doi.org/10.1093/femsec/fiv018>
- Grewer, D. M., Lafreniere, M. J., Lamoureux, S. F., & Simpson, M. J. (2016). Redistribution of soil organic matter by permafrost disturbance in the Canadian high Arctic. *Biogeochemistry*, *128*(3), 397–415. <https://doi.org/10.1007/s10533-016-0215-7>
- Helms, J. R., Stubbins, A., Ritchie, J. D., Minor, E. C., Kieber, D. J., & Mopper, K. (2008). Absorption spectral slopes and slope ratios as indicators of molecular weight, source, and photobleaching of chromophoric dissolved organic matter. *Limnology and Oceanography*, *53*(3), 955–969. <https://doi.org/10.4319/lo.2008.53.3.0955>

- Hertkorn, N., Ruecker, C., Meringer, M., Gugisch, R., Frommberger, M., Perdue, E. M., et al. (2007). High-precision frequency measurements: Indispensable tools at the core of the molecular-level analysis of complex systems. *Analytical and Bioanalytical Chemistry*, 389(5), 1311–1327. <https://doi.org/10.1007/s00216-007-1577-4>
- Hobbie, S. E., Schimel, J. P., Trumbore, S. E., & Randerson, J. R. (2000). Controls over carbon storage and turnover in high-latitude soils. *Global Change Biology*, 6(5), 196–210. <https://doi.org/10.1046/j.1365-2486.2000.06021.x>
- Hodgkins, S. B., Tfaily, M. M., Podgorski, D. C., McCalley, C. K., Saleska, S. R., Crill, P. M., et al. (2016). Elemental composition and optical properties reveal changes in dissolved organic matter along a permafrost thaw chronosequence in a subarctic peatland. *Geochimica et Cosmochimica Acta*, 187, 123–140. <https://doi.org/10.1016/j.gca.2016.05.015>
- Jin, H. J., Zhao, L., Wang, S. L., & Guo, D. X. (2006). Evolution of permafrost and environmental changes of cold regions in eastern and interior Qinghai-Tibetan Plateau since the Holocene. *Quaternary Science*, 26(2), 198–210.
- Jobbágy, E. G., & Jackson, R. B. (2000). The vertical distribution of soil organic carbon and its relation to climate and vegetation. *Ecological Applications*, 10(2), 423–436. [https://doi.org/10.1890/1051-0761\(2000\)010%5B0423:TVDOSO%5D2.0.CO;2](https://doi.org/10.1890/1051-0761(2000)010%5B0423:TVDOSO%5D2.0.CO;2)
- Kaiser, N. K., Quinn, J. P., Blakney, G. T., Hendrickson, C. L., & Marshall, A. G. (2011). A novel 9.4 tesla FTICR mass spectrometer with improved sensitivity, mass resolution, and mass range. *Journal of the American Society for Mass Spectrometry*, 22(8), 1343–1351. <https://doi.org/10.1007/s13361-011-0141-9>
- Kellerman, A. M., Dittmar, T., Kothawala, D. N., & Tranvik, L. J. (2014). Chemodiversity of dissolved organic matter in lakes driven by climate and hydrology. *Nature Communications*, 5, 3804. <https://doi.org/10.1038/ncomms4804>
- Kellerman, A. M., Kothawala, D. N., Dittmar, T., & Tranvik, L. J. (2015). Persistence of dissolved organic matter in lakes related to its molecular characteristics. *Nature Geoscience*, 8(6), 454–457. <https://doi.org/10.1038/ngeo2440>
- Koch, B. P., & Dittmar, T. (2006). From mass to structure: An aromaticity index for high-resolution mass data of natural organic matter. *Rapid Communications in Mass Spectrometry*, 20(5), 926–932. <https://doi.org/10.1002/rcm.2386>
- Lal, R. (2005). Forest soils and carbon sequestration. *Forest Ecology and Management*, 220(1–3), 242–258. <https://doi.org/10.1016/j.foreco.2005.08.015>
- Liu, X. D., & Chen, B. D. (2000). Climatic warming in the Tibetan plateau during recent decades. *International Journal of Climatology*, 20(14), 1729–1742. [https://doi.org/10.1002/1097-0088\(20001130\)20:14%3C1729::AID-JOC556%3E3.0.CO;2-Y](https://doi.org/10.1002/1097-0088(20001130)20:14%3C1729::AID-JOC556%3E3.0.CO;2-Y)
- Love, G. D., Snape, C. E., & Jarvis, M. C. (1992). Determination of the aromatic lignin content in oak wood by quantitative solid state <sup>13</sup>C-NMR. *Biopolymers*, 32(9), 1187–1192. <https://doi.org/10.1002/bip.360320908>
- Mann, P. J., Davydova, A., Zimov, N., Spencer, R. G. M., Davydov, S., Bulygina, E., et al. (2012). Controls on the composition and lability of dissolved organic matter in Siberia's Kolyma River basin. *Journal of Geophysical Research*, 117, G01028. <https://doi.org/10.1029/2011JG001798>
- Maxwell, B. (1992). Arctic climate: Potential for change under global warming. In *Arctic Ecosystems in a Changing Climate: An Ecophysiological Perspective* (pp. 11–34). San Diego, CA: Academic Press. <https://doi.org/10.1016/B978-0-12-168250-7.50008-0>
- McKnight, D. M., Boyer, E. W., Westerhoff, P. K., Doran, P. T., Kulbe, T., & Andersen, D. T. (2001). Spectrofluorometric characterization of dissolved organic matter for indication of precursor organic material and aromaticity. *Limnology and Oceanography*, 46(1), 38–48. <https://doi.org/10.4319/lo.2001.46.1.0038>
- Minor, E. C., Swenson, M. M., Mattson, B. M., & Oyler, A. R. (2014). Structural characterization of dissolved organic matter: A review of current techniques for isolation and analysis. *Environmental Science: Processes and Impacts*, 16(9), 2064–2079.
- Mu, C., Zhang, T., Zhang, X., Li, L., Guo, H., Zhao, Q., et al. (2016). Carbon loss and chemical changes from permafrost collapse in the northern Tibetan Plateau. *Journal of Geophysical Research: Biogeosciences*, 121, 1781–1791. <https://doi.org/10.1002/2015JG003235>
- Mueller, C. W., Rethemeyer, J., Kao-Kniffin, J., Löppmann, S., Hinkel, K. M., & Bockheim, J. G. (2015). Large amounts of labile organic carbon in permafrost soils of northern Alaska. *Global Change Biology*, 21(7), 2804–2817. <https://doi.org/10.1111/gcb.12876>
- Nelson, P. N., & Baldock, J. A. (2005). Estimating the molecular composition of a diverse range of natural organic materials from solid-state <sup>13</sup>C NMR and elemental analyses. *Biogeochemistry*, 72(1), 1–34. <https://doi.org/10.1007/s10533-004-0076-3>
- Obernosterer, I., & Benner, R. (2004). Competition between biological and photochemical processes in the mineralization of dissolved organic carbon. *Limnology and Oceanography*, 49(1), 117–124. <https://doi.org/10.4319/lo.2004.49.1.0117>
- Pautler, B. G., Simpson, A. J., McNally, D. J., Lamoureux, S. F., & Simpson, M. J. (2010). Arctic permafrost active layer detachments stimulate microbial activity and degradation of soil organic matter. *Environmental Technology*, 44(11), 4076–4082. <https://doi.org/10.1021/es903685j>
- Pries, C. E. H., Schuur, E. A. G., & Crummer, K. G. (2012). Holocene carbon stocks and carbon accumulation rates altered in soils undergoing permafrost thaw. *Ecosystems*, 15(1), 162–173. <https://doi.org/10.1007/s10021-011-9500-4>
- Qu, B., Sillanpää, M., Li, C., Kang, S., Stubbins, A., Yan, F., et al. (2017). Aged dissolved organic carbon exported from rivers of the Tibetan plateau. *PLoS One*, 12(5), e0178166. <https://doi.org/10.1371/journal.pone.0178166>
- Schuur, E. A. G., Abbott, B., & Permafrost Carbon, N. (2011). High risk of permafrost thaw. *Nature*, 480(7375), 32–33. <https://doi.org/10.1038/480032a>
- Schuur, E. A. G., McGuire, A. D., Schadel, C., Grosse, G., Harden, J. W., Hayes, D. J., et al. (2015). Climate change and the permafrost carbon feedback. *Nature*, 520(7546), 171–179. <https://doi.org/10.1038/nature14338>
- Serreze, M. C., & Barry, R. G. (2011). Processes and impacts of Arctic amplification: A research synthesis. *Global and Planetary Change*, 77(1–2), 85–96. <https://doi.org/10.1016/j.gloplacha.2011.03.004>
- Sjögersten, S., Caul, S., Daniell, T. J., Jurd, A. P. S., O'Sullivan, O. S., Stapleton, C. S., & Titman, J. J. (2016). Organic matter chemistry controls greenhouse gas emissions from permafrost peatlands. *Soil Biology and Biochemistry*, 98, 42–53. <https://doi.org/10.1016/j.soilbio.2016.03.016>
- Sjögersten, S., Turner, B. L., Mahieu, N., Condron, L. M., & Wookey, P. A. (2003). Soil organic matter biochemistry and potential susceptibility to climatic change across the forest-tundra ecotone in the Fennoscandian mountains. *Global Change Biology*, 9(5), 759–772. <https://doi.org/10.1046/j.1365-2486.2003.00598.x>
- Spencer, R. G. M., Guo, W., Raymond, P. A., Dittmar, T., Hood, E., Fellman, J., & Stubbins, A. (2014). Source and biolability of ancient dissolved organic matter in glacier and lake ecosystems on the Tibetan plateau. *Geochimica et Cosmochimica Acta*, 142, 64–74. <https://doi.org/10.1016/j.gca.2014.08.006>
- Spencer, R. G. M., Mann, P. J., Dittmar, T., Eglinton, T. I., McIntyre, C., Holmes, R. M., et al. (2015). Detecting the signature of permafrost thaw in Arctic rivers. *Geophysical Research Letters*, 42, 2830–2835. <https://doi.org/10.1002/2015GL063498>
- Stedmon, C. A., & Bro, R. (2008). Characterizing dissolved organic matter fluorescence with parallel factor analysis: A tutorial. *Limnology and Oceanography: Methods*, 6(11), 572–579. <https://doi.org/10.4319/lom.2008.6.572>
- Stubbins, A., Mann, P. J., Powers, L., Bittar, T. B., Dittmar, T., McIntyre, C. P., et al. (2017). Low photolability of yedoma permafrost dissolved organic carbon. *Journal of Geophysical Research: Biogeosciences*, 122, 200–211. <https://doi.org/10.1002/2016JG003688>

- Stubbins, A., Spencer, R. G. M., Chen, H. M., Hatcher, P. G., Mopper, K., Hernes, P. J., et al. (2010). Illuminated darkness: Molecular signatures of Congo River dissolved organic matter and its photochemical alteration as revealed by ultrahigh precision mass spectrometry. *Limnology and Oceanography*, *55*(4), 1467–1477. <https://doi.org/10.4319/lo.2010.55.4.1467>
- Stuiver, M., & Polach, H. A. (1977). Reporting of C-14 data—Discussion. *Radiocarbon*, *19*(03), 355–363. <https://doi.org/10.1017/S0033822200003672>
- Vonk, J. E., Tank, S. E., Bowden, W. B., Laurion, I., Vincent, W. F., Alekseychik, P., et al. (2015). Reviews and syntheses: Effects of permafrost thaw on Arctic aquatic ecosystems. *Biogeosciences*, *12*(23), 7129–7167. <https://doi.org/10.5194/bg-12-7129-2015>
- Vonk, J. E., Tank, S. E., Mann, P. J., Spencer, R. G. M., Treat, C. C., Striegl, R. G., et al. (2015). Biodegradability of dissolved organic carbon in permafrost soils and aquatic systems: A meta-analysis. *Biogeosciences*, *12*(23), 6915–6930. <https://doi.org/10.5194/bg-12-6915-2015>
- Waldrop, M. P., Wickland, K. P., White Iii, R., Berhe, A. A., Harden, J. W., & Romanovsky, V. E. (2010). Molecular investigations into a globally important carbon pool: Permafrost-protected carbon in Alaskan soils. *Global Change Biology*, *16*(9), 2543–2554.
- Wang, S. L. (1989). Formation and evolution of permafrost on the Qinghai-Xizang Plateau since the last pleistocene. *Journal of Glaciology and Geocryology*, *11*(1), 69–75.
- Wang, Y., Wang, H., He, J.-S., & Feng, X. (2017). Iron-mediated soil carbon response to water-table decline in an alpine wetland. *Nature Communications*, *8*, 15972. <https://doi.org/10.1038/ncomms15972>
- Ward, C. P., & Cory, R. M. (2015). Chemical composition of dissolved organic matter draining permafrost soils. *Geochimica et Cosmochimica Acta*, *167*, 63–79. <https://doi.org/10.1016/j.gca.2015.07.001>
- Ward, C. P., & Cory, R. M. (2016). Complete and partial photo-oxidation of dissolved organic matter draining permafrost soils. *Environmental Technology*, *50*(7), 3545–3553. <https://doi.org/10.1021/acs.est.5b05354>
- Weishaar, J. L., Aiken, G. R., Bergamaschi, B. A., Fram, M. S., Fujii, R., & Mopper, K. (2003). Evaluation of specific ultraviolet absorbance as an indicator of the chemical composition and reactivity of dissolved organic carbon. *Environmental Technology*, *37*(20), 4702–4708. <https://doi.org/10.1021/es030360x>
- Yang, Y., Ji, C., Chen, L., Ding, J., Cheng, X., & Robinson, D. (2015). Edaphic rather than climatic controls over <sup>13</sup>C enrichment between soil and vegetation in alpine grasslands on the Tibetan Plateau. *Functional Ecology*, *29*(6), 839–848. <https://doi.org/10.1111/1365-2435.12393>
- Zhang, Y. C. S. (1981). Discussion on the time of formation of permafrost on Qingzang Plateau. *Journal of Glaciology and Geocryology*, (1), 32–37.
- Zhang, X., Hutchings, J. A., Bianchi, T. S., Liu, Y., Arellano, A. R., & Schuur, E. A. (2017). Importance of lateral flux and its percolation depth on organic carbon export in Arctic tundra soil: Implications from a soil leaching experiment. *Journal of Geophysical Research: Biogeosciences*, *122*, 796–810. <https://doi.org/10.1002/2016JG003754>